Chemical Methodologies 9(2025) 277-300

Chemical Methodologies

Journal homepage: http://chemmethod.com

Original Article

In Depth *in Silico* Exploration of Some Natural Indole Alkaloids as Potential Plasmepsin II Inhibitors: ADMET Calculations, Molecular Docking Analysis, Molecular Dynamics Simulation, and DFT Studies

Konatham Teja Kumar Reddy[1,*], Uppuluri Varuna Naga Venkata Arjun[2], Jehad F. Alhmoud[3], S. Mounika Reddy[4], Dhillishree D.[2], Vishal B. Tambe[5], Ganesh S. Shinde[5], Thukani Sathanantham Shanmugarajan[2,*], G. Dharmamoorthy[6], Gobalakriahnan P.[7]

[1]*Department of Pharmacy, University College of Technology, Osmania University, Amberpet, Hyderabad, Telangana 500007, India*
[2]*Department of Pharmaceutics, School of Pharmaceutical Sciences, Vels Institute of Science, Technology and Advanced Studies (VISTAS). PV Vaithiyalingam Rd, Velan Nagar, Krishna Puram, Pallavaram, Chennai, 600117, Tamil Nadu, India*
[3]*Department of Medical Laboratory Sciences, Jordan University of Science and Technology, P.O. Box 3030, Irbid, 22110, Jordan*
[4]*Department of Pharmaceutics, Malla Reddy Institute of Pharmaceutical sciences, Hyderabad, Telangana, India*
[5]*Pravara Rural Education Society's Institute of Pharmacy Loni, Rahata, Loni Bk., Maharashtra 413736, India*
[6]*Department of Pharmaceutical Analysis, MB School of Pharmaceutical Sciences, Mohan Babu University (Erstwhile Sree Vidyaniketan College of Pharmacy) Tirupati, India*
[7]*Department of Pharmaceutical Chemistry, Vagdevi College of Pharmacy and Research centre, Nellore, Andhra Pradesh, India*

ARTICLEINFO

Article history
Submitted: 2025-01-16
Revised: 2025-02-17
Accepted: 2025-02-21
ID: CHEMM-2501-1884

DOI: 10.48309/CHEMM.2025.500292.1884

KEYWORDS
Plasmepsin II
Antimalarial
Natural alkaloids
Molecular docking
MDS
ADMET

ABSTRACT

Plasmepsin II, an aspartic protease enzyme found in the malarial parasite Plasmodium falciparum, plays a critical role in malaria pathogenesis. Quinine, quinidine, cinchonine, and cinchonidine are four quinoline alkaloids derived from Cinchona officinalis bark that have a human malaria cure rate exceeding 98%. In terms of intra-erythrocytic malarial parasites, quinine is schizonticidal and gametocytocidal for *Plasmodium vivax* and *Plasmodium malaria*, whereas it has no effect on P. falciparum gametocytes. Therefore, this study investigates natural indole alkaloids as potential inhibitors of Plasmepsin II for treating P. falciparum malaria. The ADMET profiles of the selected indole alkaloids were calculated and the binding affinity of the ligand with Plasmepsin II was determined. The Desmond program ran a molecular dynamic simulation (MDS) at 100 ns to verify the stability and function of the complex in a physiological-chemical environment. Ergocornine and native ligands were analyzed using density functional theory (DFT) calculations to evaluate their electronic properties and reactivity. In ADMET Screening, all the screened compounds displayed optimum ADMET profiles to be developed or treated as lead nuclei for further study. In computational screening, the native ligand displayed -7.5 kcal/mol of binding free energy, while most potent compound such as Ergocornine exhibited -9.5 kcal/mol binding affinity. MDS analysis showed that the complex displayed a very stable conformation and demonstrated compact ligand binding. DFT studies indicated that Ergocornine exhibited higher stability and lower reactivity compared to the native ligand, highlighting its potential for therapeutic applications. These natural alkaloids may possess potential anti-plasmepsin II activity, which can be further investigated using numerous *in vitro* or *in vivo* models. We aim to report this finding in the future.

* Corresponding author: Konatham Teja Kumar Reddy; Thukani Sathanantham Shanmugarajan
E-mail: teja.konatham1704@gmail.com; mailshanmuga@gmail.com

GRAPHICAL ABSTRACT

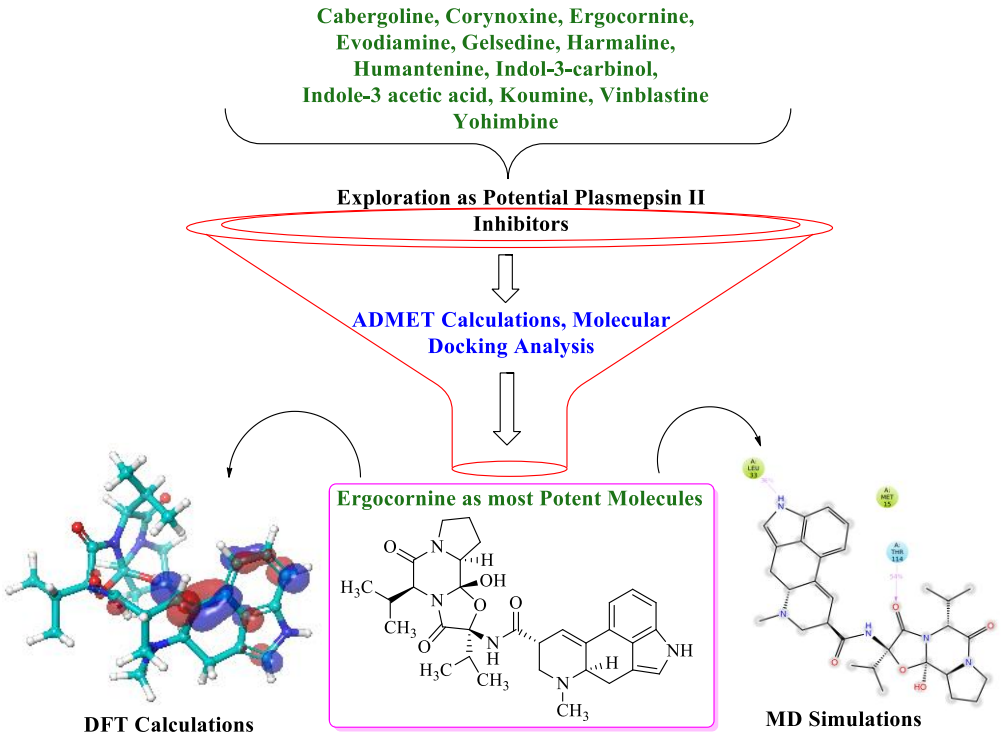

Introduction

Plasmepsin II, an aspartic protease enzyme, was isolated from the malaria parasite *Plasmodium falciparum (P. falciparum)* [1]. The human body requires proteolytic digestion to break down hemoglobin. By inhibiting plasmepsin II, the parasite fails to degrade hemoglobin, leading to the accumulation of toxic heme metabolites that kill the parasite [2,3]. Extensive research on plasmepsin II inhibitors has identified and characterized various small molecules as potential antimalarial drugs [4-6]. Biochemical and cell-based experiments have demonstrated that multiple chemical classes—including peptidomimetics, transition state analogs, and natural products—can effectively inhibit plasmepsin II. Peptidomimetic inhibitors competitively bind to the active site of plasmepsin II, preventing hemoglobin cleavage. Both *in vitro* and *in vivo* studies have demonstrated the strong antimalarial properties of these inhibitors, which halt the maturation of parasites and significantly increase survival rates in malaria-infected animals. It has become easier to find and improve lead compounds that can block plasmepsin II owing to progress in the structural basis of drug design and high-throughput screening. However, *P. falciparum* and other species continue to pose significant challenges to the development of plasmepsin II inhibitors as antimalarial drugs [7]. To ensure the clinical efficacy of plasmepsin II inhibitors, it is crucial to address challenges such as drug resistance, pharmacokinetic variability, and toxicological profiles. Despite these hurdles, plasmepsin II inhibitors hold promise as novel antimalarial agents with the potential to contribute significantly to global malaria eradication efforts. A large number of quinolone-based antimalarial medicines can be prepared using indole alkaloids as guide templates. Among the several classes of alkaloids present, steroidal alkaloids, bisbenzylisoquinolines, naphthylisoquinolines, indoloquinolines, and indolomonoterpenoid alkaloids exhibit the highest antiparasitic and antiplasmodial activity [8]. Cinchona officinalis bark yields four quinoline alkaloids: quinine, quinidine, and cinchonine, with a cure rate for malaria in humans exceeding 98% (see Figure 1). Quinine remains a first-line antimalarial drug for the treatment of severe malaria because of its resistance [9].

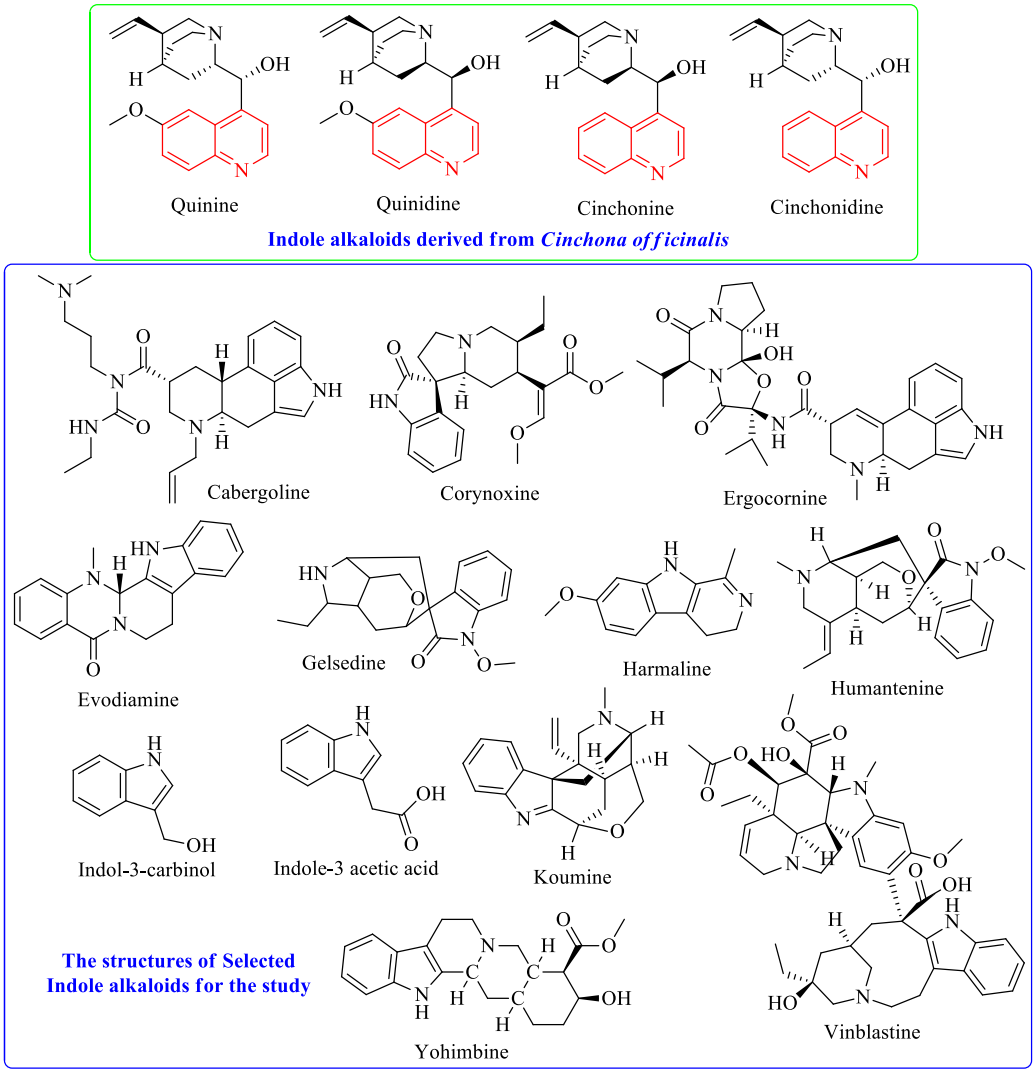

Figure 1: The structures of indole alkaloids derived from *Cinchona officinalis* which has antimalarial activity and the indole alkaloids selected for the study

The Schizontocidal effectiveness of quinine against intraerythrocytic malarial parasites is as follows: it effectively inhibits the gametocytes of *Plasmodium vivax* and *Plasmodium malaria*, while it has no effect on *P. falciparum*. Therefore, in the present study, we have investigated some natural indole alkaloids as potential Plasmepsin II inhibitors, in the hope to be used against malaria caused by *P. falciparum*.

Experimental

ADMET Properties Calculations

ADMETlab 2.0 (https://admetmesh.scbdd.com/) was employed to determine the absorption, distribution, metabolism, excretion, and toxicity (ADMET) properties of all selected indole alkaloids [10]. It is an online web server designed to calculate the drug-likeness properties of designed molecules. The results of ADMET properties were compared with the properties of native ligand.

Computational Analysis

The binding affinities (docking scores) are determined by molecular docking algorithms that assess the interaction energy between a ligand and a target protein. These values generally include Van der Waals forces, electrostatic interactions, hydrogen bonding, and de-solvation effects. A decreased binding energy signifies a heightened binding affinity, indicating a more potent interaction. A significantly negative docking score often indicates enhanced binding

stability and possible biological efficacy. The binding affinity of the ligand for Plasmepsin II was determined using the AutoDock Vina version present in the PyRx Virtual Screening tool [11]. The structures of the selected indole alkaloids have been provided in the graphical abstract. ChemDraw Ultra 12.0 helped all ligands to be drawn structurally and stored in MOL file format, which maintains atomic coordinates, bonding data, and molecular characteristics. This guarantees compatible representation and accuracy for further computational investigation [12]. The crystalline structure of *P. falciparum* plasmepsin II bound to the inhibitor PG418 (~{N}1-[(~{Z},3~{R})-4-[2-(3-methoxyphenyl)propan-2-ylamino]-3-oxidanyl-1-phenyl-but-1-en-2-yl]-5-piperidin-1-yl-~{N}3,~{N}3-dipropyl-benzene-1,3-dicarboxamide) was obtained from the official Protein Data Bank website (https://www.rcsb.org/structure/4y6m) [13]. The PDB code for this enzyme is 4Y6M. The target was purified using Biovia Discovery Studio Visualizer, and the ligand-binding domain (LBD) was identified [14-15]. The same cavity dimensions were used to perform the docking studies (center_x = 29.8651531632, center_y = -32.1459009331, center_z = -35.8606169117; size_x = 26.5908666361; size_y = 15.0656091944; size_z = 18.6265748602). All ligands, including the native ligand and the target, were imported into the PyRx virtual screening tool and subjected to docking studies. The ligands were subjected for energy minimization followed by converting them into pdbqt file format. The energy minimization was performed by universal force field (UFF). Interactions were analyzed using the Biovia Discovery Studio [16-19]. The 3D ribbon view of the enzyme with the native ligand present in the LBD is depicted in Figure 2.

Molecular Dynamic Simulations

To verify the stability and function of the complex in a physiological-chemical environment, the Desmond program ran a molecular dynamic simulation at 100 ns. The complex used in the simulation was derived from the first docking results, which provided binding interaction analyses for both static and rigid modes. The molecular dynamic (MD) simulation process revealed binding and further interaction analyses in a physicochemical environment during the simulation [20]. Preprocess, refine, and optimize the complex using Maestro's Protein Preparation Wizard. The complex was set up and the energy required to run the simulation was reduced using the system builder model. To simulate typical physiological circumstances in the human body, we selected pressure (1 atm) and temperature (310 K).

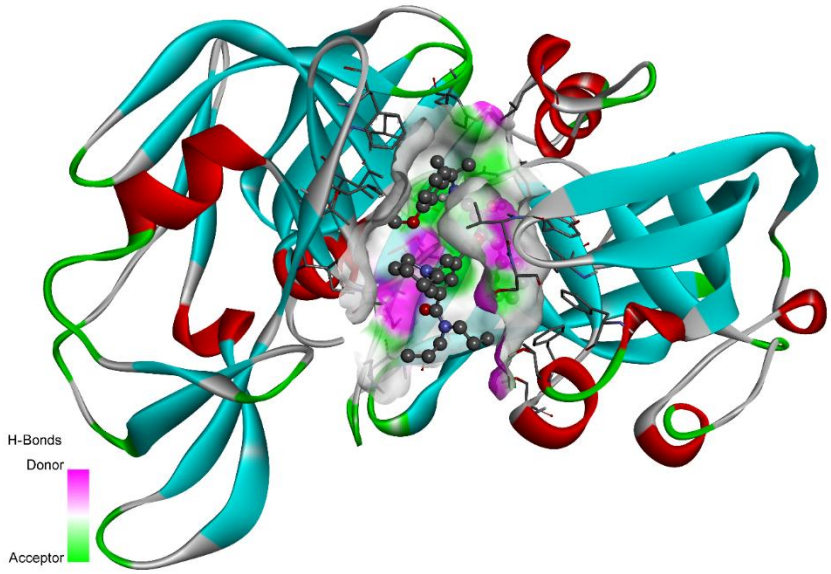

Figure 2: 3D ribbon representation of plasmepsin II (PDB ID: 4Y6M) with its native ligand bound in the ligand-binding domain (LBD)

Selected for its general applicability and confirmed accuracy in MDS to replicate water behavior was the TIP3P (Intermolecular Interaction Potential 3 Points Transferable) solvent model. To guarantee a medically appropriate environment, 0.15 M sodium chloride was further supplied to simulate physiological ionic strength. The excluded region was measured as 20 Å. The trajectory of the simulation at 100 ns is recorded every 100 ps [16]. The 100 ns simulation duration was chosen as it is widely used in MDS studies to capture significant conformational changes and stabilize protein-ligand interactions. This timeframe ensures reliable analysis while balancing computational efficiency. In addition, prior studies on similar systems support its adequacy for observing relevant MD. The analysis encompassed various aspects of the MD trajectory, including root mean square deviation (RMSD), Root Mean Square Fluctuation (RMSF), and protein secondary structure.

Density Functional Theory (DFT) Calculations

The representative compounds Ergocornine and Native ligands were subjected to in-depth evaluation using advanced theoretical quantum calculations. These calculations employed DFT calculations within the Jaguar platform. The B3LYP method, incorporating Becke's three-parameter exchange potential and the Lee-Yang-Parr correlation functional, was applied along with the 6-21G** basis set to predict the molecular properties. The 6-21G** basis set was chosen as a computationally efficient option for initial quantum calculations, balancing accuracy and resource demands. While larger basis sets like 6-31G or cc-pVTZ offer improved precision, 6-21G** provides reliable molecular property predictions for our system. The analysis explored key quantum chemical attributes, including the Frontier Molecular Orbital (FMO) theory, which examines the characteristics of the highest occupied molecular orbital (HOMO) and the lowest unoccupied molecular orbital (LUMO) [21-22]. The HOMO and the LUMO are essential in DFT analyses, since they reflect a molecule's electronic characteristics, reactivity, and stability. A reduced HOMO-LUMO gap indicates increased chemical reactivity and possible bioactivity, affecting molecular interactions in pharmaceutical design. These characteristics facilitate the prediction of binding affinity, charge transfer, and the overall potential of a chemical as a therapeutic agent. Furthermore, global reactivity parameters were calculated to provide critical insights into molecular reactivity and stability.

Results and Discussion

ADMET Properties

The discovery and development of novel medications heavily depends on the processes of chemical absorption, distribution, metabolism, and excretion, collectively referred to as ADMET [23]. An ideal drug candidate must exhibit not only sufficient efficacy against the therapeutic target, but also superior ADMET characteristics at the therapeutic dosage. To evaluate the potential of the compound, researchers conducted a comprehensive analysis to assess its toxicity, drug-likeness, and ADME profile [16,23]. To further support medicinal chemists in the lead optimization process, a novel approach called *in silico* ADMET assessment models has been developed. These models enable researchers to examine the biological effects of potential pharmaceutical candidates by predicting their pharmacokinetic properties. Understanding and optimizing these pharmacokinetic qualities are crucial for the development of novel medications, as they significantly influence drug efficacy, safety, and overall success in clinical trials [24]. Table 1 presents the calculated physicochemical properties of the indole alkaloids and native ligands. The analysis revealed that most compounds adhered to acceptable ranges of molecular weight (MW), hydrogen bond acceptors (nHAs), hydrogen bond donors (nHDs), rotatable bonds (nRots), Van der Waals (vdW) volumes, and total polar surface areas (TPSAs).

Table 1: Physicochemical properties of indole alkaloids

Code	Physicochemical Properties							
	Molecular Weight	Volume	nHA	nHD	nRot	TPSA	logS	logP
NL	640.400	696.384	8	3	17	94.140	-3.881	6.190
Cabergoline	451.290	478.135	7	2	11	71.680	-2.333	3.357
Corynoxine	384.200	396.178	6	1	5	67.870	-3.710	2.969
Ergocornine	561.300	562.680	10	3	5	118.210	-3.217	3.804
Evodiamine	303.140	315.087	4	1	0	39.340	-5.435	3.106
Gelsedine	328.180	332.216	5	1	2	50.800	-3.370	2.192
Harmaline	214.110	225.336	3	1	1	37.380	-3.268	2.954
Humantenine	354.190	364.172	5	0	1	42.010	-4.117	2.844
Indol-3-carbinol	147.070	156.349	2	2	1	36.020	-1.664	1.390
Indole-3 acetic acid	175.060	179.798	3	2	2	53.090	-2.107	1.762
Koumine	306.170	320.739	3	0	1	24.830	-4.038	2.724
Vinblastine	810.420	821.262	13	3	10	154.100	-4.756	4.059
Yohimbine	354.190	364.172	5	2	2	65.560	-2.907	2.662

However, exceptions were noted for the native ligands Ergocornine, and Vinblastine, which exceeded the recommended MW threshold of 500 Da. In addition, Vinblastine surpassed the acceptable limit of 13 nHAs. The lipophilicity of a drug, represented by the logP and logS values, plays a pivotal role in determining various pharmacokinetic properties, including solubility, absorption, membrane permeability, plasma protein binding, distribution, and tissue penetration [25]. Recognizing the critical importance of lipophilicity, the Lipinski rule of five was expanded to incorporate both the logP and logS parameters [25]. In the present study, all examined parameters were within suitable ranges and demonstrated optimal oral bioavailability. This suggested that the studied compounds may be amenable to oral administration. A comprehensive analysis of these physicochemical properties provides valuable insights into the potential drug-like characteristics of indole alkaloids and native ligands, providing a foundation for the further development and optimization of these compounds as potential therapeutic agents [26-27].

Table 2 lists the drug-like characteristics of these ligands. Several parameters were evaluated, including the quantitative estimate of drug-likeness (QED), natural product-likeness score (NPscore), Lipinski rule (MW of < 500 Da, LogP of ≤ 5, hydrogen bond donors (HBD) of ≤ 5, and hydrogen bond acceptors (HBA) of ≤ 10.), Pfizer rule [LogP ≤ 3, HBD ≤ 3, and (ClogP × PSA) < 75], GSK rule, Golden Triangle, and Chelator rule. The QED, introduced in 2012, serves as a metric for determining drug likeness based on data from existing marketed medications. In modern drug discovery, computational tools and evaluation of drug-like properties are widely employed in the development of small-molecule therapeutics. All the ligands examined in this study exhibited favorable QED values [28-29]. According to the Pfizer rule, compounds with log P values exceeding 3 and topological polar surface areas (TPSA) below 75 $Å^2$ are likely to exhibit toxicity [30]. According to the GSK rule, molecules with a molecular mass below 400 and CLogP value below 4 are more likely to exhibit an ideal ADME profile [31]. Using *in vitro* permeability, *in vitro* clearance, and computational data, the Golden Triangle (200 ≤ MW ≤ 50; -2 ≤ logD ≤ 5) was created as a visualization tool to help medicinal chemists discover drug candidates that are metabolically stable, permeable, and powerful [32]. The current study revealed that the native ligand and Vinblastine did not comply with Lipinski's rule. Regarding the Pfizer rule, Cabergoline, Ergocornine, and Evodiamine failed to meet these criteria. The GSK rule was not satisfied by the native ligands Cabergoline, Ergocornine, and Vinblastine.

Table 2: Drug-likeness properties of indole alkaloids

Code	Medicinal Chemistry						
	QED	NPscore	Lipinski Rule	Pfizer Rule	GSK Rule	Golden Triangle	Chelator Rule
NL	0.173	-1.059	Rejected	Accepted	Rejected	Rejected	0
Cabergoline	0.605	0.028	Accepted	Rejected	Rejected	Accepted	0
Corynoxine	0.491	1.881	Accepted	Accepted	Accepted	Accepted	0
Ergocornine	0.526	1.427	Accepted	Rejected	Rejected	Accepted	0
Evodiamine	0.692	0.166	Accepted	Rejected	Accepted	Accepted	0
Gelsedine	0.902	2.512	Accepted	Accepted	Accepted	Accepted	0
Harmaline	0.778	0.723	Accepted	Accepted	Accepted	Accepted	0
Humantenine	0.727	2.771	Accepted	Accepted	Accepted	Accepted	0
Indol-3-carbinol	0.632	0.300	Accepted	Accepted	Accepted	Rejected	0
Indole-3 acetic acid	0.731	-0.105	Accepted	Accepted	Accepted	Rejected	0
Koumine	0.745	2.565	Accepted	Accepted	Accepted	Accepted	0
Vinblastine	0.180	1.533	Rejected	Accepted	Rejected	Accepted	0
Yohimbine	0.773	1.091	Accepted	Accepted	Accepted	Accepted	0

Table 3: An absorption parameters of indole alkaloids

Code	Absorption						
	Caco-2 Permeability	MDCK Permeability	Pgp-inhibitor	Pgp-substrate	HIA	F20%	F30%
NL	-5.590	1.3e-05	+++	++	---	--	--
Cabergoline	-5.463	5.3e-06	---	+++	---	---	---
Corynoxine	-4.525	3.7e-05	---	+	---	+	+++
Ergocornine	-5.237	1.3e-05	+++	--	---	+++	+++
Evodiamine	-4.797	2.4e-05	+++	+++	---	---	--
Gelsedine	-4.907	8.5e-05	++	---	---	----	---
Harmaline	-5.123	1.7e-05	+	+++	---	++	---
Humantenine	-4.999	3.3e-05	++	++	---	--	-
Indol-3-carbinol	-4.411	9.5e-06	---	---	---	---	+++
Indole-3 acetic acid	-4.501	1.5e-05	---	---	---	---	---
Koumine	-5.205	3.2e-05	---	+++	---	---	+++
Vinblastine	-5.615	1.3e-05	++	+++	+++	+++	+++
Yohimbine	-4.957	1.1e-05	---	+++	---	---	---

The Golden Triangle rule was not met by the native ligands Indol-3-carbinol, and Indole-3 acetic acid. Collectively, these results suggest the favorable ADMET characteristics of the compounds. Failing to meet these drug-like criteria may indicate poor absorption, distribution, metabolism, or toxicity issues, potentially reducing a compound's efficacy and safety. Such deviations can lead to poor bioavailability or off-target effects, necessitating further optimization to enhance drug-likeness and therapeutic potential. Absorption parameters play a crucial role in drug development by providing valuable insights into the extent to which a drug enters the bloodstream after administration. By understanding these criteria, such as drug solubility and intestinal permeability, scientists can predict the efficacy of treatment in the human body. Optimizing these absorption coefficients can enhance the likelihood of medications to exhibit efficacy and safety when administered. Table 3 presents a visual representation of the absorption properties of indole alkaloids. The

Caco-2 cell line, derived from human colon epithelial carcinoma, serves as a representative model for studying drug absorption in the digestive system. This approach is particularly useful for predicting the intestinal permeability and drug efflux. Notably, all compounds exhibited the highest possible Caco-2 permeability, which was achieved when the value exceeded -4.358 log [33]. MDCK-MDR1 facilitates researchers in obtaining a more comprehensive understanding of medication efflux and provides early indications of potential drug permeability issues. Studies have demonstrated that the MDCK-MDR1 permeability serves as a reliable predictor of blood-brain barrier permeability, thus complementing the permeability of the intestinal barrier [34]. Several compounds exhibited Pgp-substrate and Pgp-inhibitor activities. Only Vinblastine exhibits good intestinal absorption in humans (HIA). The metabolic profiles and chemical distributions of these ligands are listed in Table 4. Several compounds exhibited plasma protein binding (PPB) below 90%, indicating that highly protein-bound medications may have a limited therapeutic range. The volume distribution (VD) for all compounds was within the acceptable range (optimal range: 0.04-20 L/kg). The Blood-Brain Barrier (BBB) is a specialized network of Brain Micro-vascular Endothelial Cells (BMVEC) that safeguards the brain from harmful substances in the bloodstream while ensuring that essential nutrients reach the brain tissues. Owing to its restricted permeability, the BBB poses a significant challenge in delivering therapeutic agents to the Central Nervous System (CNS) [35].

Table 4: Distribution and metabolism profile of indole alkaloids

Code	Distribution				Metabolism									
					CYP1A2		CYP2C19		CYP2C9		CYP2D6		CYP3A4	
	PPB (%)	VD	BBB Penetration	Fu	Inhibitor	Substrate	Inhibitor	Substrate	Inhibitor	Substrate	Inhibitor	Substrate	Inhibitor	Substrate
NL	96.817	1.197	+++	1.412	--	+++	+	-	+	--	-	++	+++	++
Cabergoline	48.948	2.153	+++	63.449	---	-	---	++	---	--	++	++	--	+++
Corynoxine	63.658	1.183	+++	30.886	---	++	+	+++	-	--	+++	++	+++	+++
Ergocornine	90.457	2.831	--	2.649	---	---	-	++	++	---	---	--	+++	+++
Evodiamine	94.049	1.049	++	3.059	++	++	+++	-	++	++	--	++	++	-
Gelsedine	14.102	1.510	++	73.255	---	++	--	+++	---	--	---	+	+	+++
Harmaline	86.413	1.473	+++	12.601	+++	+++	--	++	---	+++	++	+++	---	-
Humantenine	48.638	2.309	+++	35.062	---	+	---	+++	---	--	--	+	+	+++
Indol-3-carbinol	51.033	1.021	++	37.448	+++	++	-	-	---	++	+	++	---	--
Indole-3 acetic acid	79.148	0.251	-	12.501	--	--	---	---	---	+++	---	+	---	--
Koumine	63.45	2.883	+++	35.446	--	+	---	+++	---	--	++	++	++	+++
Vinblastine	77.363	1.936	--	19.369	---	+++	----	+++	---	---	+++	++	+++	+++
Yohimbine	57.851	1.924	+	40.931	-	+++	---	++	---	--	--	++	--	++

All ligands demonstrated blood-brain barrier (BBB) penetration potential, except for Ergocornine, indole-3-acetic acid, and Vinblastine. Being a substrate or inhibitor of cytochrome enzymes enhances drug activity because of their role in drug metabolism [36-37]. Interactions involving Cytochrome P450 alter medication metabolism, impacting clearance rates, bioavailability, and possible toxicity. Inhibitors may decelerate metabolism, resulting in elevated drug concentrations and potential deleterious consequences, while substrates may vie for enzymatic processing, so modifying effectiveness. Polymorphisms in CYP enzymes may influence individual responses, requiring dosage modifications for individualized therapy.

Table 5 provides a thorough summary of the excretion and toxicity profiles of all ligands examined. The majority of compounds exhibited low-to-moderate clearance rates, with Ergocornine being the exception at 15.608 16.265 mL/min/kg. All ligands demonstrated short half-lives, with $T_{1/2}$ values of < 3 h. The under-study compounds generally showed favorable toxicity characteristics. This characteristic highlights the majority of ligands exhibiting low cytotoxicity, mutagenicity, or organ toxicity risks. Providing this data strengthens the claim and supports their potential for further drug development. However, Ergocornine, Evodiamine, Indole-3 acetic acid, and Koumine are associated with drug-induced liver injury. The Ames assay, also known as bacterial reverse mutation assay, is a widely accepted and reliable method for evaluating chemical mutagens. This technique assesses their capacity to restore the ability of mutant *Salmonella typhimurium* and/or *Escherichia coli* to produce amino acids [38]. This study revealed that Gelsedine and Humantenine exhibit Ames toxicity, suggesting their mutagenic nature. The mutagenic potential of Gelsedine and Humantenine, as shown by the Ames assay, raises questions about their safety and regulatory approval. Mutagenicity may result in genetic instability and possible carcinogenic hazards, requiring further *in vitro* and *in vivo* verification.

Table 5: Excretion and toxicity profile of indole alkaloids

Code	Excretion		Toxicity									
	Cl	T1/2	H-HT	DILI	AMES Toxicity	Rat Oral Acute Toxicity	FDAMDD	Skin Sensitization	Carcinogencity	Eye Corrosion	Eye Irritation	Respiratory Toxicity
NL	3.943	0.327	++	--	---	++	-	-	---	---	---	+++
Cabergoline	6.646	0.686	-	-	--	++	+++	+	---	---	---	+++
Corynoxine	12.066	0.209	+	-	-	+++	+++	+++	+++	---	---	+++
Ergocornine	15.608	0.841	--	+++	---	+	+++	--	+++	---	---	++
Evodiamine	3.795	0.431	+	+++	---	+++	+++	++	++	---	-	+++
Gelsedine	7.366	0.048	--	--	++	+	+++	-	++	---	---	++
Harmaline	8.992	0.334	-	--	---	+++	+++	++	--	--	++	+++
Humantenine	14.565	0.159	-	-	+	-	++	-	++	---	---	+++
Indol-3-carbinol	8.384	0.922	--	-	--	++	--	+	--	---	+++	+
Indole-3 acetic acid	7.532	0.920	--	+++	---	+	---	-	--	---	+++	--
Koumine	7.236	0.079	+	++	--	+++	+++	+	-	---	---	+++
Vinblastine	2.188	0.017	++	---	--	+++	+++	---	---	---	---	+++
Yohimbine	8.862	0.426	-	---	---	+	+++	--	--	---	---	+++

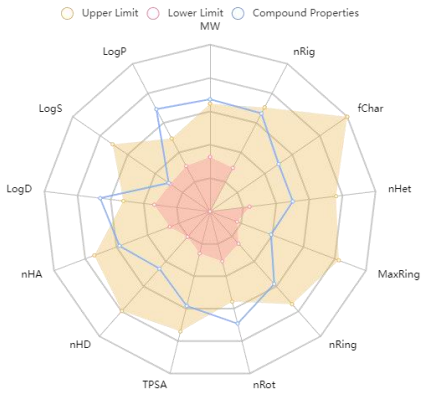

Native ligand

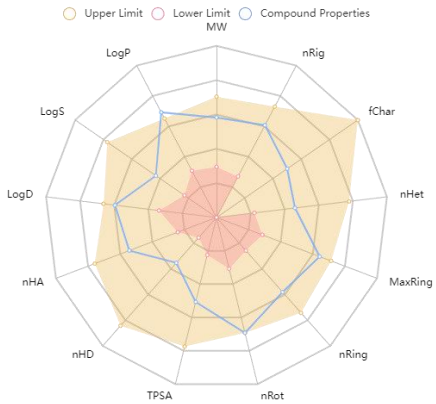

Cabergoline

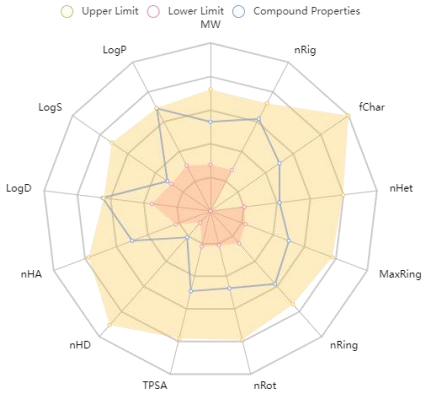

Corynoxine

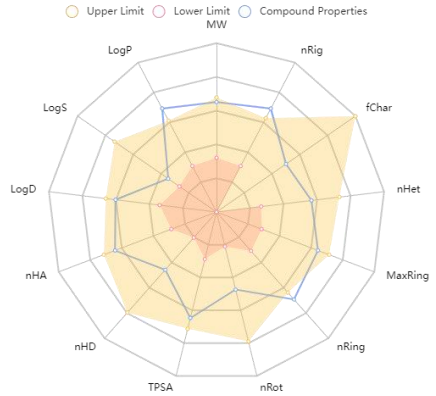

Ergocornine

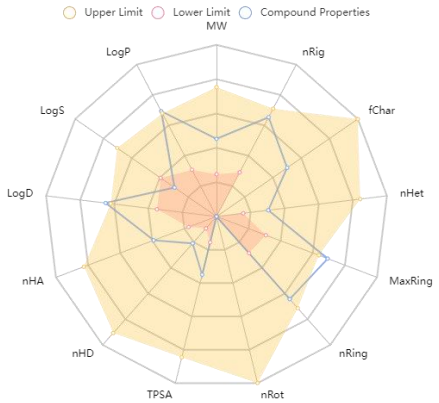

Evodiamine

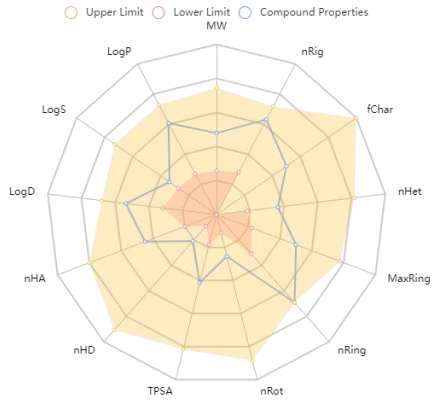

Gelsedine

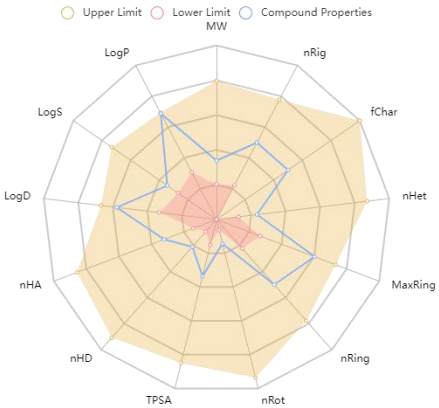

Harmaline

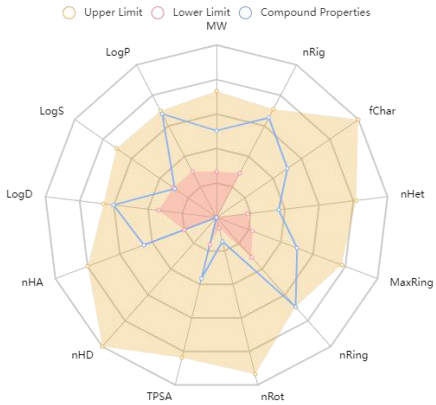

Humantenine

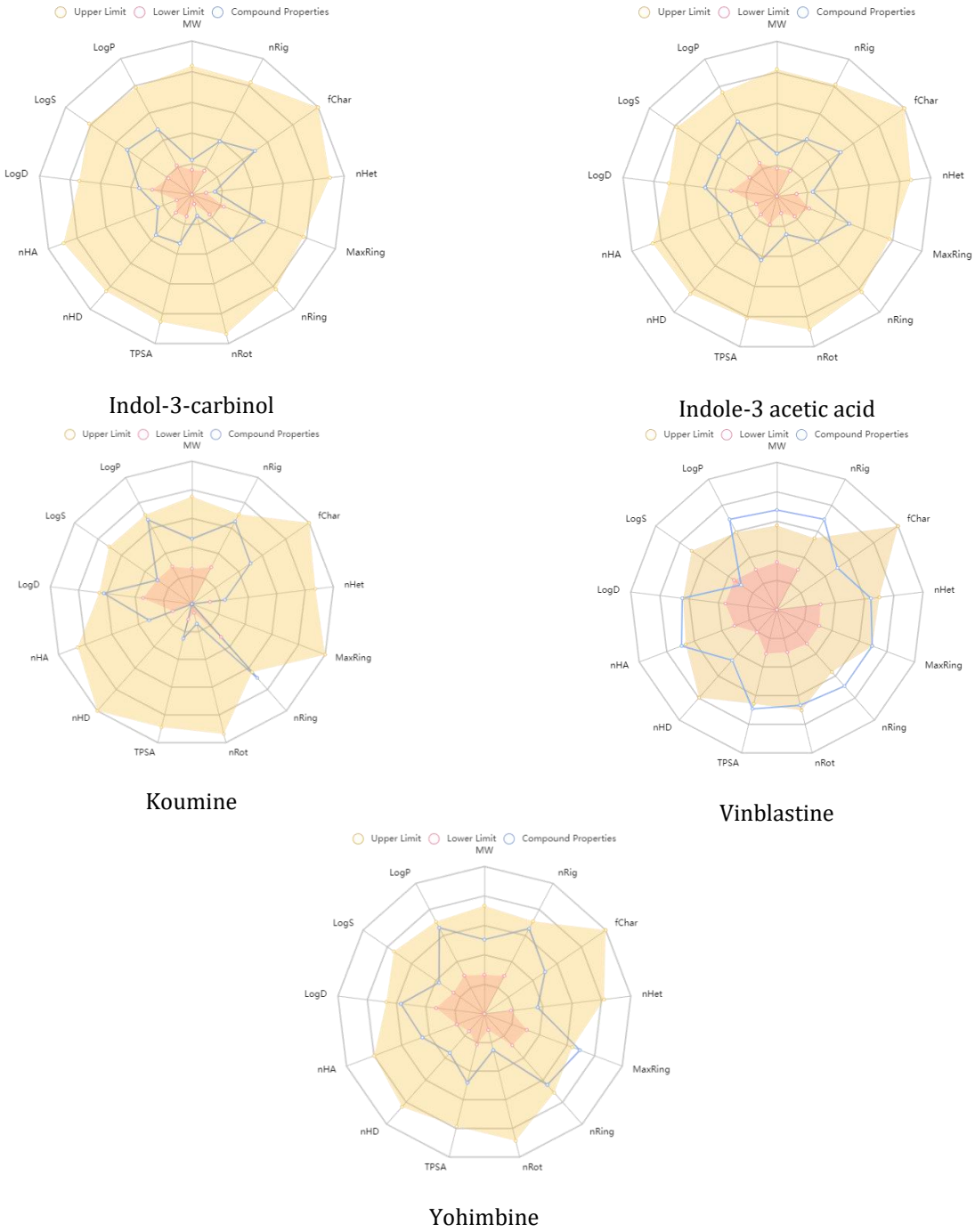

Figure 3: The physicochemical radar of the indole alkaloids

Upon confirmation, their therapeutic development may need structural alterations, rigorous dose restrictions, or other formulations to reduce hazards. Moreover, regulatory obstacles may need comprehensive genotoxicity assessments prior to clinical advancement. The physicochemical characteristics of the ligands are demonstrated in Figure 3. This profile emphasizes the favorable physicochemical attributes of the compounds, which could inform their subsequent development [10]. The bio-concentration factors (IGC50, LC50FM, and LC50DM) provide essential information on the environmental persistence and bioaccumulation potential of the examined compounds. Elevated readings suggest an increased probability of bioaccumulation in aquatic species, presenting ecological hazards and possible toxicity issues. Comprehending these aspects aids in evaluating long-term environmental safety and adherence to regulations.

Table 6: Environmental toxicity profile of indole alkaloids

Name	Environmental toxicity			
	Bio-concentration Factors	IGC_{50}	$LC_{50}FM$	$LC_{50}DM$
NL	1.232	4.950	5.245	5.434
Cabergoline	0.299	2.408	5.619	5.144
Corynoxine	0.352	2.650	3.237	5.068
Ergocornine	0.170	2.301	4.516	4.785
Evodiamine	1.063	2.117	4.578	5.112
Gelsedine	1.616	3.287	3.884	4.301
Harmaline	0.825	3.407	3.827	5.693
Humantenine	1.687	4.515	5.226	4.622
Indol-3-carbinol	0.461	2.492	3.812	4.780
Indole-3 acetic acid	0.311	2.540	3.308	4.108
Koumine	2.363	4.397	5.686	5.530
Vinblastine	0.851	4.175	4.922	5.049
Yohimbine	0.611	2.758	3.781	5.957

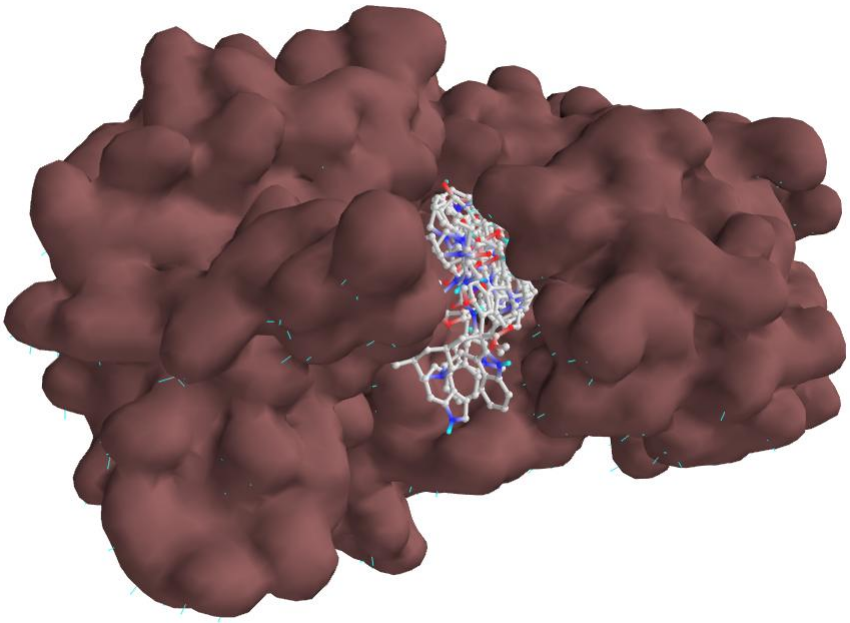

Figure 4: The combined docking view of the molecules entrapped in LBD of the target (4Y6M)

If substantial bioaccumulation is detected, further biodegradability studies and risk evaluations may be necessary to guarantee sustainable pharmaceutical use [39-42]. Table 6 provides the environmental toxicity profile of the molecules, presenting bio-concentration factors, including IGC_{50}, $LC_{50}FM$, and $LC_{50}DM$.

Computational Analysis

Using molecular docking, researchers can create new medicines faster, increase their efficacy, and reduce toxicity. This technique allows evaluation of the potential activity of ligands against biological targets by virtually screening all compounds. Figure 4 depicts the combined docking view of the synthesized 3D structures of these molecules superimposed within the LBD of the target molecule. Figures 5 and 6 show the 3D and 2D-molecular interaction poses of most potent compounds with targeted protein. The molecular interactions of these compounds are listed in Table S1, and their 2D binding poses are depicted in Figure S1 of the Supplementary Information.

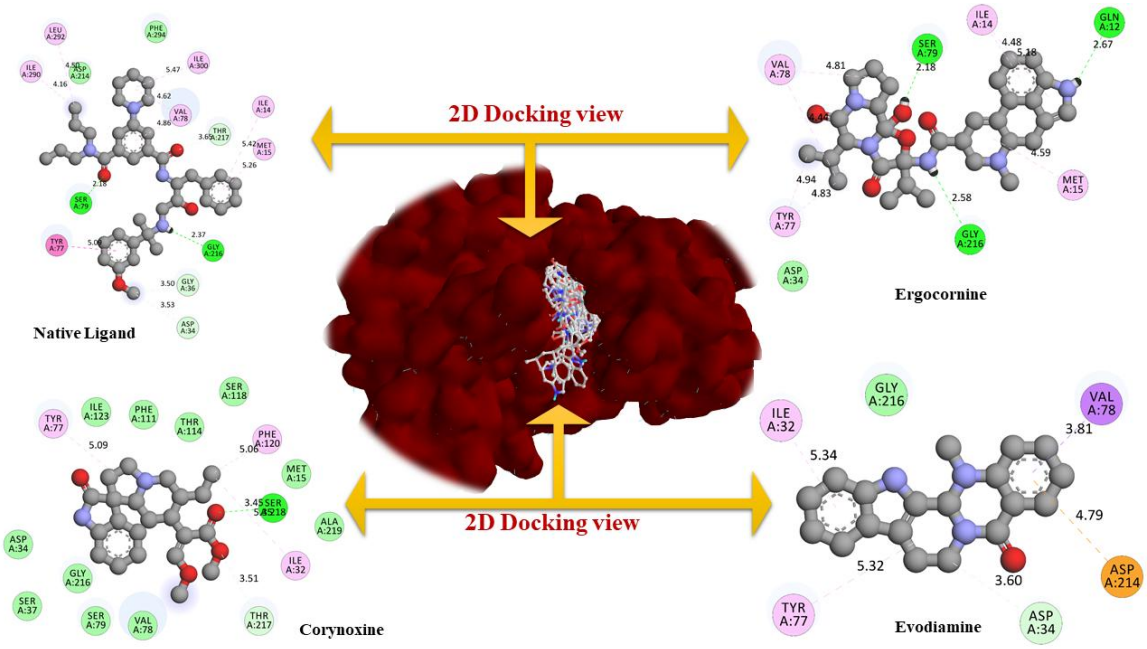

Figure 5: The 3D and 2D-molecular interaction poses of native ligand, Corynoxine, Ergocornine, and Evodiamine with targeted protein

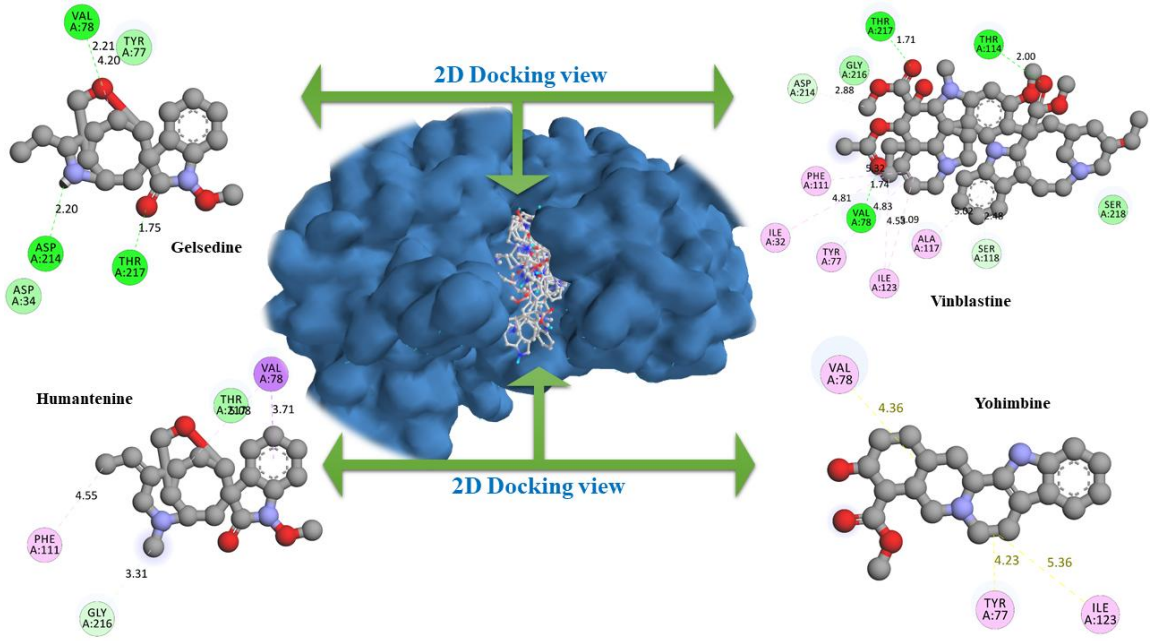

Figure 6: The 3D and 2D-molecular interaction poses of Gelsedine, Humantenine, Vinblastin, and Yohimbin with targeted protein

A molecular docking study of natural indole alkaloids as potential Plasmepsin II inhibitors revealed intriguing details about how these molecules interact with the enzyme's active site [43]. The compounds included in this study were Cabergoline, Corynoxine, Ergocornine, Evodiamine, Gelsedine, Harmaline, Humantenine, Indole-3-Carbinol, Indole-3-Acetic Acid, Koumine, Vinblastine, and Yohimbine. It was observed that various compounds involved the same amino acid residues in their binding interactions. The native ligand was used as a benchmark to compare the binding interactions of other compounds with Plasmepsin II. For Cabergoline, we observed strong hydrogen-bonding interactions with SER79, THR217, TYR192, and GLY216. We also

observed electrostatic interactions with ASP214, and hydrophobic interactions with VAL78, ILE123, and PHE111. These are the key residues, SER218 and THR217, along with ILE32, TYR77, and PHE120, which establish hydrogen bonds with Corynoxine and engage in strong hydrophobic bonds with GLY216, GLN12, and SER79. Ergocornine also has many hydrophobic interactions with VAL78, MET15, ILE14, and TYR77. There were four types of interactions between ASP214 and Evodiamine. ASP34 forms a carbon-hydrogen bond with Evodiamine, VAL78 and ILE32 share hydrophobic interactions, and TYR77 also forms hydrophobic interactions. Gelsedine forms strong hydrogen bonds with ASP214, VAL78, and THR217. It also forms hydrophobic bonds with VAL78 and formed hydrogen bonds with ASP34 and hydrophobic interactions with VAL78. GLY216 formed a carbon-hydrogen bond with Humantenine and a hydrophobic interaction with VAL78 and PHE111. Indole-3-carbinol interacts with the hydrophobic regions of ILE123, TYR77, and ILE32. It formed hydrogen bonds with ASP214, THR217, ASP34, and GLY216. Furthermore, it prevents water molecules from interacting with ILE123, TYR77, or ILE32. KOUMINE forms hydrogen bonds with ASP34 and hydrophobic interactions with TYR77, ILE32, and VAL78. Vinblastine exhibited strong hydrogen bonding interactions with VAL78, THR114, THR217, ASP214, and SER118, along with numerous hydrophobic interactions with ILE123, ILE32, ALA117, TYR77, and PHE111. They suggested that Yohimbine forms hydrophobic interactions with ILE123, VAL78, and TYR77. In particular, the binding of most of the examined alkaloids appeared to be VAL78-dependent [44-45].

The remaining residues bind to several compounds, such as Ergocornine, Cabergoline, Corynoxine, Gelsedine, Harmaline, Humanine, Koumine, Vinblastine, and Yohimbine. VAL78's apparent frequent involvement makes it essential for the design of potential inhibitors of plasmepsin-II attachment. TYR77 is a residue found in several other proteins. It interacts with the native ligand and several compounds; for example, ILE32 interacts with Corynoxine, Evodiamine, Indole-3-Carbinol, Indole-3-Acetic Acid, Koumine, and Vinblastine. However, the recurrent presence of these residues in various compounds suggests their importance in the binding mechanism of Plasmepsin II inhibitors. ASP214 and a higher-affinity THR217 site frequently interact with Cabergoline, Gelsedine, indole-3-acetic acid, and Vinblastine. Some of these residues may contribute to stabilizing potential interactions with ligands or forming hydrogen bonds. For example, certain compounds exhibit unique interaction patterns. For example, a wider range of residues (THR114, SER118, ALA117, and PHE111) interacted with Vinblastine than with the other compounds. Therefore, Vinblastine may bind more complexly or occupy a larger part of the binding pocket. Residues involved in native ligand interactions were GLY216, SER79, ASP34, and GLY36 [46].

Overall, Ergocornine and Vinblastine showed the most promising interactions among the tested compounds and may be leading candidates for Plasmepsin II inhibition. We examined the binding patterns of the investigated alkaloids in comparison with those of the native ligand, potentially providing clues into their efficacy as inhibitors. However, it is important to note that although these interaction patterns provide some insights into the binding modes of these natural indole alkaloids, none of them definitively indicate their potential for inhibition. Finding real drugs, especially those that block Plasmepsin II, depend on the stability of the protein-ligand complex and the effectiveness of the experiments. In this study, we conducted MDS to investigate the stability of protein-ligand complexes.

Molecular Dynamics Simulation (MDS)

The computer route was employed to examine a 100-ns simulation of the protein-Ergocornine complex. The analysis encompassed various aspects of the MD trajectory, including RMSD, RMSF, and protein secondary structure [47]. A comprehensive investigation of the material's interactions with the protein revealed the substance's adhesion and engagement with the target during the simulation period.

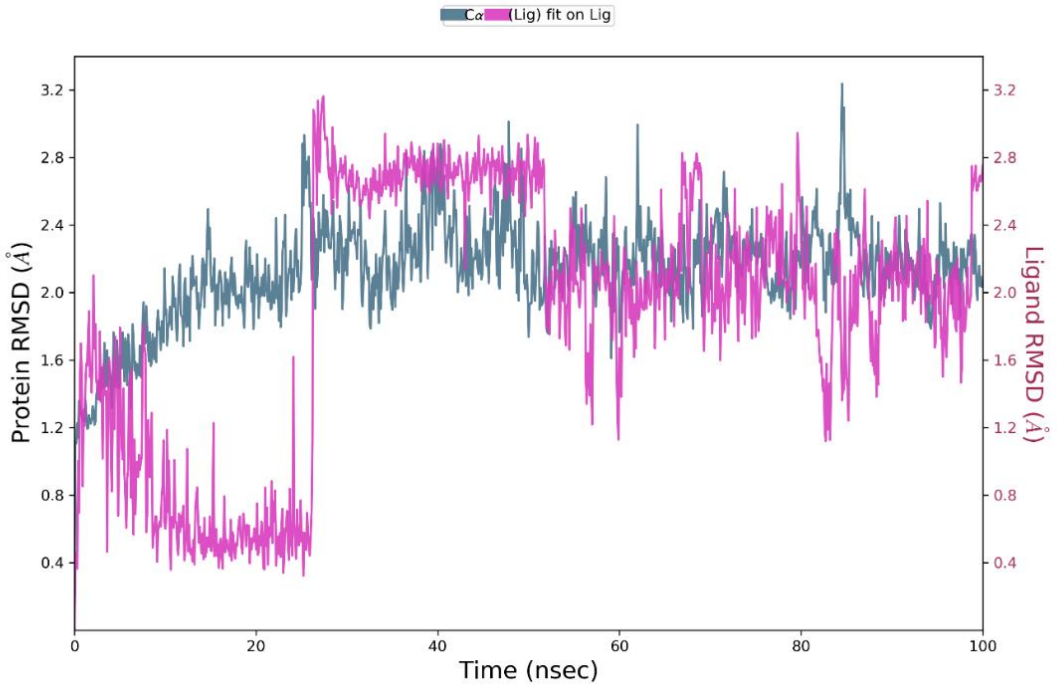

Figure 7: Time-dependent RMSD of C-alpha atoms in ligands and proteins. Whereas the right Y-axis displays changes in ligand RMSD over time, the left Y-axis shows changes in protein RMSD over time

This meticulous examination provided valuable insights into the behavior of the compound and its potential as a therapeutic candidate, facilitating the assessment of its stability, binding characteristics, and suitability for further investigation. The stability of the simulation was evaluated by comparing the RMSD of the ligand and protein over time [47-48].

Figure 7 illustrates the temporal changes in RMSD values for the C-alpha atoms of ligand-bound proteins. RMSD in molecular dynamics simulations quantifies the structural changes of a protein from its initial configuration. As illustrated in Figure 7, the protein structure was stabilized at approximately 10 ns. Throughout the experiment, the RMSD values varied within a range of 1.0 Angstrom, with a slight fluctuation at 80ns that remained under 1.5 Angstrom [49]. The protein exhibited a strong bond with the ligand, as evidenced by RMSD [47-48,50]. Conformational changes in the bonds, potentially caused by ligand rotation, could explain this shift. Such alterations are typically attributed to changes in the ligand torsion angle. The protein-ligand complex showed a minor increase in RMSD at 25 ns. The RMSD of the ligand in the complex reached equilibrium within the first 5ns and maintained stability for 25 ns. The slight increase observed at 25 ns could be due to a conformational shift in the bonds, possibly resulting from the ligand rotation. These shifts are often associated with changes in the ligand torsion angle. RMSD analysis concluded that the protein-ligand complex achieved a stable state [49]. Despite some fluctuations, both the protein and ligand maintained their structural integrity throughout the simulation. This stability suggests that the protein structure is suitable for further investigation.

Figure 8 illustrates the RMSF values for the protein-ligand complex. These values indicate the extent to which specific amino acid residues in the protein complex deviated from their average positions during the molecular dynamics simulation. Analysis of the simulation trajectories revealed that residues exhibiting higher RMSF plot peaks are typically found in flexible regions, such as loops or the C and N-terminal ends of the protein, suggesting increased structural variability and dynamic activity in these areas.

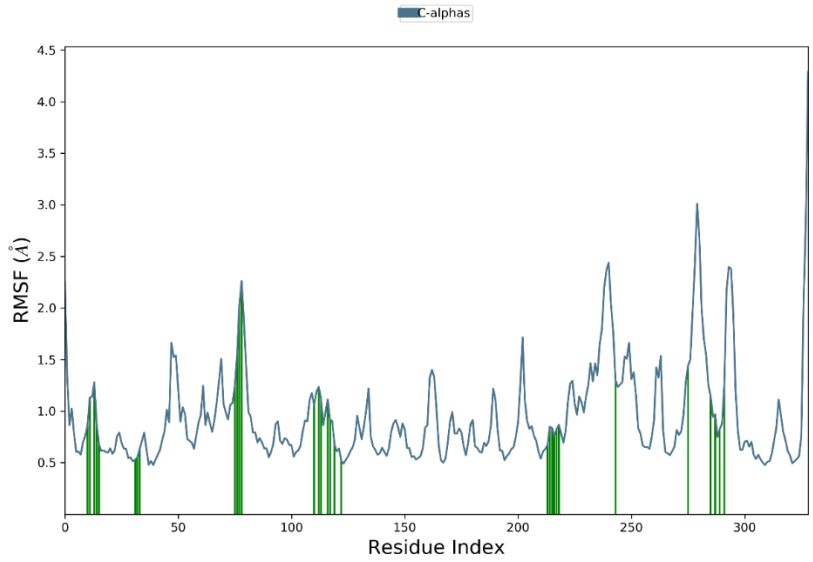

Figure 8: Residue wise RMSF of protein-ligand complexed

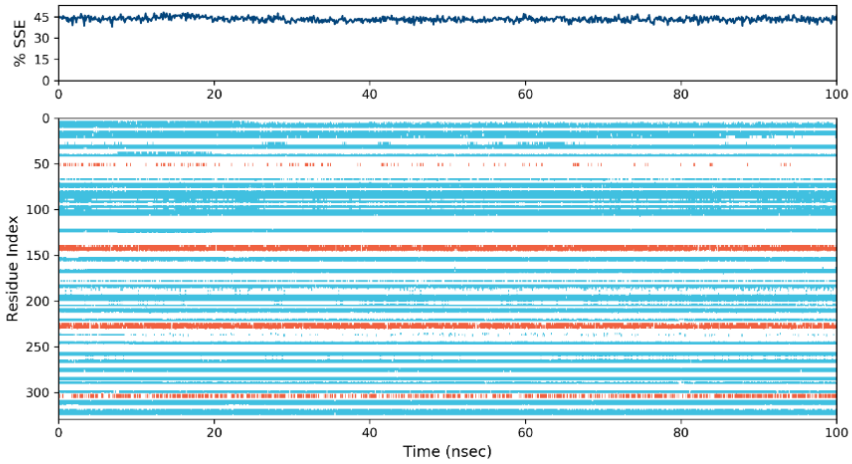

Figure 9: The way how the locations of each residue in protein-ligand interactions affect the distribution of secondary protein structure components. To be more precise, beta strands denoted by blue columns and alpha helices by red ones

The RMSF values of amino acids at the ligand-binding site were examined to determine the stability of ligand binding to the protein [51]. Lower RMSF values for particular binding site residues indicated reduced variability in ligand-protein interactions throughout the simulation. Figure 9 depicts the distribution of secondary structural elements (SSE) within the protein during the simulation. The arrangement of beta and alpha helices within the protein structure is graphically represented, with the distribution mapped against the residue index. Visualization displayed the position of these structural elements within the protein by aligning the SSE with each residue index. Figure 10 shows that the predominant interactions between the ligand and protein during molecular dynamics (MD) are hydrogen bonds and hydrophobic interactions. These interactions are vital for maintaining stability and facilitating ligand-protein binding. Specifically, hydrogen bonding is essential for interactions between certain amino acids and ligands. The key amino acids involved in hydrogen bonding included LEU_33, THR_114, and SER_218, whereas ILE_14, MET_15, ILE_32, VAL_78, PHE_111, and ALA-117 were significant for hydrophobic interactions.

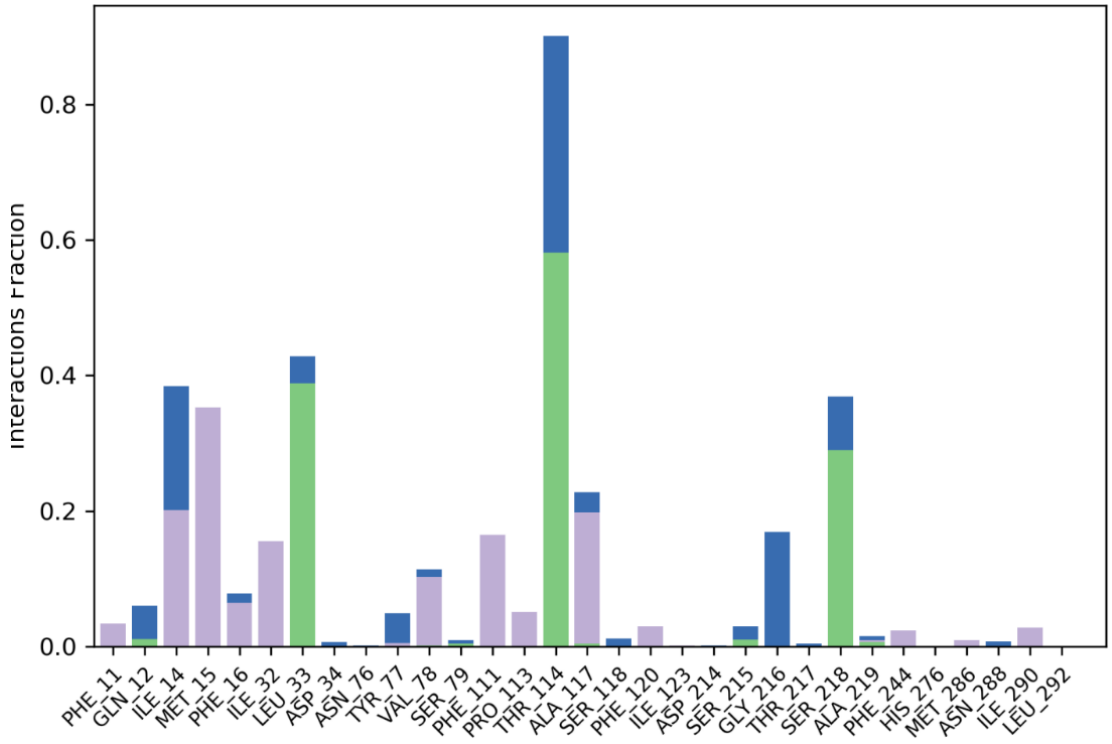

Figure 10: Heatmap of protein-ligand interaction throughout trajectory

These amino acids exhibit a high propensity to form hydrogen bonds and hydrophobic interactions, which are crucial for effective attachment of the ligand to the protein. The timeline chart in Figure 4 depicts the dynamic changes in ligand-protein contacts and connections throughout the experiment. This timeline enables researchers to observe the timing and nature of these critical interactions during simulation, offering valuable insights into complex dynamics and stabilization.

Figure 9 emphasizes the significance of hydrogen bonds in ligand-protein interactions, highlighting specific amino acids whose binding function relies on hydrogen bonding. The timeline display enhances the understanding of the complex behavior during MD simulation by providing a dynamic view of the evolution of these interactions.

DFT Calculations

DFT has proven to be a powerful tool in drug discovery and design for evaluating the electronic properties and chemical reactions of compounds. DFT provides valuable insights into the reactivity and stability of molecules by focusing on the HOMO and LUMO energy levels. In this study, the Becke, 3-parameter, Lee-Yang-Parr (B3LYP) functional was utilized to investigate the electronic structure and behavior of the compounds. Frontier molecular orbitals, namely the HOMO and LUMO, were analyzed, as they are critical in determining the chemical reactivity and kinetic stability. The HOMO serves as an electron donor, acting as a nucleophile, whereas the LUMO functions as an electron acceptor, acting as an electrophile. The energy difference (ΔE) between the HOMO and LUMO was calculated, as it plays a vital role in assessing the molecular stability. A larger ΔE indicates greater stability and reduced chemical reactivity, which are key factors in the development of drug candidates with desirable properties. Furthermore, the electronic absorption characteristics were interpreted as one-electron transitions from the HOMO to LUMO, reflecting excitation from the ground state to the first excited state [52-54]. The DFT analysis highlighted that both compounds under study (Ergocornine and native ligand) demonstrated significant reactivity, reflected in their electronic properties and ΔE values.

Table 7: DFT-based frontier molecular orbital energies (eV) and global reactivity parameters

Code	Ergocornine	Native ligand
HOMO	-0.198	-0.290
LUMO	-0.032	-0.143
ΔE	0.166	0.147
Ionization potential (IP)	0.198	0.290
Electron affinity (EA)	0.032	0.143
electronegativity (X)	0.115	0.217
Chemical hardness (η)	0.083	0.074
Chemical softness (S)	6.028	6.801
Chemical potential (μ)	0.115	0.217
Electrophilic index (ω)	0.080	0.320

Chemical hardness (η) = (IP - EA) / 2; chemical potential (μ) = − (IP + EA) / 2; electronegativity (χ) = (IP + EA) / 2; chemical softness (S) = 1/ 2η; Electrophilic index (ω) = μ2 / 2η.

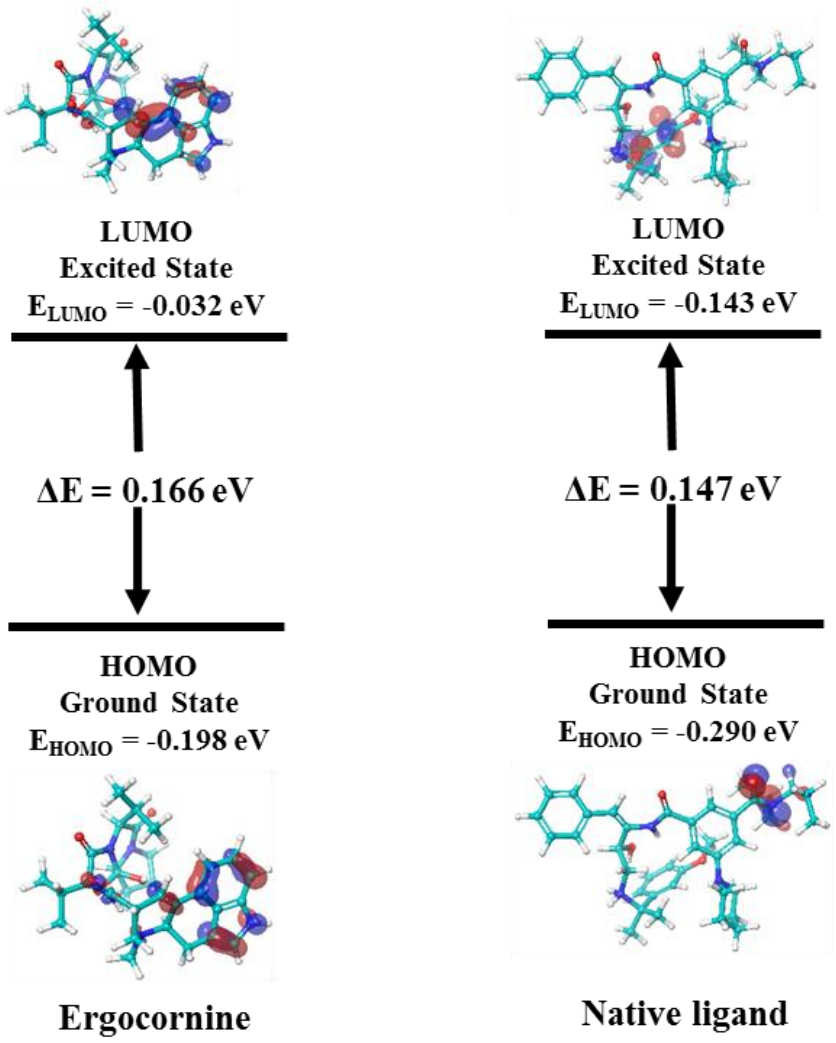

Figure 11: The HOMO and the LUMO diagram of Ergocornine and native ligand

By analyzing frontier molecular orbital energies and global reactivity parameters, it is possible to predict the stability, reactivity, and interaction potential of a compound with biological targets. The calculated parameters for Ergocornine and the native ligand (Table 7) provide valuable insights into their chemical behavior and potential for therapeutic applications. The HOMO and LUMO are essential indicators of the reactivity of a molecule. The HOMO represents

the ability of a molecule to donate electrons (nucleophilicity), while the LUMO signifies its capacity to accept electrons (electrophilicity). The energy gap (ΔE) between the HOMO and LUMO reflects the kinetic stability and chemical reactivity of the molecule, with a larger gap suggesting a higher stability and lower reactivity [55-56]. Ergocornine, with HOMO and LUMO energies of -0.198 eV and -0.032 eV, respectively, has a ΔE of 0.166 eV, which is slightly larger than the ΔE of the native ligand (0.147 eV), indicating higher stability and lower reactivity (Figure 11). Ionization potential (IP) measures the energy required to remove an electron from a molecule, whereas electron affinity (EA) represents the energy released when a molecule gains an electron. These parameters are fundamental for understanding the redox behavior of compounds. As indicated in Table 7, it was observed that, Ergocornine showed lower IP (0.198 eV) and EA (0.032 eV) than the native ligand (IP = 0.290 eV, EA = 0.143 eV), suggesting reduced electron donation and acceptance tendencies. The electronegativity (χ) and chemical potential (μ) reflect the molecule's ability to attract electrons and overall stability; the lower values of Ergocornine (χ = 0.115 eV, μ = 0.115 eV) compared to the native ligand (χ = 0.217 eV, μ = 0.217 eV) indicate less electron attractiveness and greater stability. Chemical hardness (η) and softness (S) are indicators of the resistance of a molecule to electronic deformation. A higher hardness implies greater stability, while a higher softness indicates higher reactivity. Ergocornine's higher hardness (η = 0.083 eV) and lower softness (S = 6.028 eV) than the native ligand (η = 0.074 eV, S = 6.801 eV) underscores its enhanced stability. Lastly, the electrophilicity index (ω), a measure of the ability of a molecule to accept electrons, is significantly lower for Ergocornine (ω = 0.080 eV) than for the native ligand (ω = 0.320 eV), suggesting the latter's higher reactivity and potential for electrophilic interactions. Collectively, these results highlight the greater stability and lower reactivity of Ergocornine, making it a promising candidate for drug design, while the higher reactivity of the native ligand may suit dynamic biological interactions. Ergocornine is an ergot alkaloid having diverse pharmacological effects, mostly linked to its interaction with dopamine receptors. These characteristics include dopamine agonist activity, vasoconstriction, activation of uterine contractions, and the ability to induce peripheral ischemia. Ergocornine is regarded as one of the less effective ergot alkaloids when compared to other ergot alkaloids like ergotamine and ergometrine.

Conclusion

Based on *in silico* analysis, several natural indole alkaloids have shown potential as Plasmepsin II inhibitors, which could be valuable for the development of new antimalarial treatments. Compounds such as Corynoxine, Ergocornine, Evodiamine, Gelsedine, Humantenine, Vinblastine, and Yohimbine exhibited promising binding affinity energies ranging from -7.6 to -9.5 kcal/mol, surpassing the native ligand's binding free energy of -7.5 kcal/mol. Most potent compound, Ergocornine exhibited -9.5 kcal/mol binding affinity with Plasmepsin II. Ergocornine exhibited -9.5 kca/mol of binding affinity and developed three potent conventional H-bonds with GLN12, SER79, and GLY216. It has developed many hydrophobic interactions with VAL78, MET15, ILE14, and TYR77. These findings provide valuable insights for future structure-based drug design efforts targeting Plasmepsin II. The molecular dynamics simulation conducted over 100 ns demonstrated stable protein-Ergocornine interactions, with consistent RMSD values. RMSF analysis revealed flexible protein regions and a stable ligand-binding site. This stability suggests Ergocornine forms a robust and durable interaction with Plasmepsin II. RMSD quantifies the overall structural stability of a protein-ligand complex, reflecting the extent of atomic position fluctuations over time. Reduced RMSD values imply stable binding, but higher values may indicate conformational alterations. RMSF evaluates residue-level flexibility, emphasizing areas with considerable mobility that might influence binding interactions. Collectively, these parameters provide insights

into the dynamic stability and predictability of pharmacological interactions. DFT studies indicated that Ergocornine exhibited higher stability and lower reactivity compared to the native ligand, highlighting its potential for therapeutic applications. In summary, Ergocornine showed the most favorable interactions among the compounds studied, suggesting that they may be the most promising candidates for Plasmepsin II inhibition. Although these computational results are promising, it is important to note that further *in vitro* and *in vivo* studies are necessary to validate these predictions and to assess the true potential of these natural indole alkaloids as Plasmepsin II inhibitors. We aim to report such studies in the near future to provide a more comprehensive evaluation of the potential of these compounds as antimalarial agents.

Acknowledgements

The authors are thankful to the R. C. Patel Institute of Pharmaceutical Education and Research for providing the DFT Studies of the compounds.

Please see supporting information file.

ORCID

Konatham Teja Kumar Reddy
https://orcid.org/0000-0003-0227-2248
Uppuluri Varuna Naga Venkata Arjun
https://orcid.org/0000-0001-9464-420X
Jehad F. Alhmoud
https://orcid.org/0000-0002-0010-0381
S. Mounika Reddy
https://orcid.org/0009-0004-4390-3004
Dhillishree D.
https://orcid.org/0009-0006-2423-1470
Vishal B. Tambe
https://orcid.org/0000-0002-2116-4317
Ganesh S. Shinde
https://orcid.org/0000-0003-3461-6236
Thukani Sathanantham Shanmugarajan
https://orcid.org/0000-0003-0167-4579
G. Dharmamoorthy
https://orcid.org/0009-0009-3869-9324
Gobalakriahnan P.
https://orcid.org/0009-0003-0499-4014

References

[1]. Shntaif A.H., Khan S., Tapadiya G., Chettupalli A., Saboo S., Shaikh M.S., Siddiqui F., Amara R.R., Rational drug design, synthesis, and biological evaluation of novel N-(2-arylaminophenyl)-2, 3-diphenylquinoxaline-6-sulfonamides as potential antimalarial, antifungal, and antibacterial agents, *Digital Chinese Medicine*, 2021, **4**:290 [Crossref], [Google Scholar], [Publisher]
[2]. Schneider V.M., Visone J.E., Harris C.T., Florini F., Hadjimichael E., Zhang X., Gross M.R., Rhee K.Y., Ben Mamoun C., Kafsack B.F., The human malaria parasite Plasmodium falciparum can sense environmental changes and respond by antigenic switching, *Proceedings of the National Academy of Sciences*, 2023, **120**:e2302152120 [Crossref], [Google Scholar], [Publisher]
[3]. Mori T., Nakashima M., Sequence-dependent heterochromatin formation in the human malaria parasite Plasmodium falciparum, *Heliyon*, 2023, **9** [Google Scholar], [Publisher]
[4]. Boss C., Richard-Bildstein S., Weller T., Fischli W., Meyer S., Binkert C., Inhibitors of the Plasmodium falciparum parasite aspartic protease plasmepsin II as potential antimalarial agents, *Current Medicinal Chemistry*, 2003, **10**:883 [Crossref], [Google Scholar], [Publisher]
[5]. Corminboeuf O., Dunet G., Hafsi M., Grimont J., Grisostomi C., Meyer S., Binkert C., Bur D., Jones A., Prade L., Inhibitors of Plasmepsin II—potential antimalarial agents, *Bioorganic & Medicinal Chemistry Letters*, 2006, **16**:6194 [Crossref], [Google Scholar], [Publisher]
[6]. Cheuka P.M., Dziwornu G., Okombo J., Chibale K., Plasmepsin inhibitors in antimalarial drug discovery: medicinal chemistry and target validation (2000 to present), *Journal of medicinal chemistry*, 2020, **63**:4445 [Crossref], [Google Scholar], [Publisher]
[7]. Malau N.D., Anti-malarial activity in plasmepsin ii inhibitors using molecular docking, *International Journal of Progressive Sciences and Technologies (IJPSAT)*, 2021, **27**:111 [Google Scholar], [Publisher]

[8]. Tisnerat C., Dassonville-Klimpt A., Gosselet F., Sonnet P., Antimalarial drug discovery: from quinine to the most recent promising clinical drug candidates, *Current Medicinal Chemistry*, 2022, **29**:3326 [Crossref], [Google Scholar], [Publisher]
[9]. Lakhani I, Sharma G, Alim H, Ali A, Patel N., Antioxidants from Antimalarial Plants and Their Applications. In *Antimalarial Medicinal Plants*, CRC Press. 2024, 128 [Google Scholar], [Publisher]
[10]. Xiong G., Wu Z., Yi J., Fu L., Yang Z., Hsieh C., Yin M., Zeng X., Wu C., Lu A., ADMETlab 2.0: an integrated online platform for accurate and comprehensive predictions of ADMET properties, *Nucleic Acids Research*, 2021, **49**:W5 [Crossref], [Google Scholar], [Publisher]
[11]. Eberhardt J., Santos-Martins D., Tillack A.F., Forli S., AutoDock Vina 1.2. 0: New docking methods, expanded force field, and python bindings, *Journal of Chemical Information and Modeling*, 2021, **61**:3891 [Crossref], [Google Scholar], [Publisher]
[12]. Cousins KR., Computer review of ChemDraw ultra 12.0. *Journal of the American Chemical Society,* 2011, **133**: 8388 [Google Scholar], [Publisher]
[13]. Recacha R., Leitans J., Akopjana I., Aprupe L., Trapencieris P., Jaudzems K., Jirgensons A., Tars K., Structures of plasmepsin II from Plasmodium falciparum in complex with two hydroxyethylamine-based inhibitors, *Acta Crystallographica Section F: Structural Biology Communications*, 2015, **71**:1531 [Crossref], [Google Scholar], [Publisher]
[14]. Baroroh U., Biotek M., Muscifa Z.S., Destiarani W., Rohmatullah F.G., Yusuf M., Molecular interaction analysis and visualization of protein-ligand docking using biovia discovery studio visualizer, *Indonesian Journal of Computational Biology (IJCB)*, 2023, **2**:22 [Crossref], [Google Scholar], [Publisher]
[15]. Dallakyan S., Olson A.J., Small-molecule library screening by docking with PyRx, *Chemical Biology: Methods and Protocols*, 2015, 243 [Crossref], [Google Scholar], [Publisher]
[16]. Suryawanshi R.M., Shimpi R.B., Muralidharan V., Nemade L.S., Gurugubelli S., Baig S., Vikhe S.R., Dhawale S.A., Mortuza M.R., Sweilam S.H., ADME, Toxicity, Molecular Docking, Molecular Dynamics, Glucokinase activation, DPP-IV, α-amylase, and α-glucosidase Inhibition Assays of Mangiferin and Friedelin for Antidiabetic Potential, *Chemistry & Biodiversity*, 2025, e202402738 [Crossref], [Google Scholar], [Publisher]
[17]. Vawhal P.K., Jadhav S.B., Kaushik S., Panigrahi K.C., Nayak C., Urmee H., Khan S.L., Siddiqui F.A., Islam F., Eftekhari A., Coumarin-based sulfonamide derivatives as potential DPP-IV inhibitors: Pre-ADME analysis, toxicity profile, computational analysis, and in vitro enzyme assay, *Molecules*, 2023, **28**:1004 [Crossref], [Google Scholar], [Publisher]
[18]. Khan S., Siddiqui F., Jain S., Sonwane G., Discovery of potential inhibitors of SARS-CoV-2 (COVID-19) main protease (Mpro) from Nigella Sativa (black seed) by molecular docking study, *Coronaviruses*, 2021, **2**:384 [Crossref], [Google Scholar], [Publisher]
[19]. Chaudhari R.N., Khan S.L., Chaudhary R.S., Jain S.P., Siddiqui F., B-Sitosterol: Isolation from muntingia calabura linn bark extract, structural elucidation and molecular docking studies as potential inhibitor of SARS-CoV-2 mpro (COVID-19), *Asian J. Pharm. Clin. Res*, 2020, **13**:204 [Crossref], [Google Scholar], [Publisher]
[20]. Kumar A., Singh V.K., Kayastha A.M., Molecular modeling, docking and dynamics studies of fenugreek (Trigonella foenum-graecum) α-amylase, *Journal of Biomolecular Structure and Dynamics*, 2023, **41**:9297 [Crossref], [Google Scholar], [Publisher]
[21]. Chaudhari B., Patel H., Thakar S., Ahmad I., Bansode D., Optimizing the Sunitinib for cardio-toxicity and thyro-toxicity by scaffold hopping approach, *In Silico Pharmacology*, 2022, **10**:10 [Crossref], [Google Scholar], [Publisher]
[22]. Desai N.C., Joshi S.B., Khasiya A.G., Jadeja D.J., Mehta H.K., Pandya M., Ahmad I., Patel H., Pyrazolo-imidazolidinones: Synthesis, antimicrobial assessment and molecular modelling studies by molecular mechanic and quantum mechanic approach, *Journal of Molecular Structure*, 2022, **1270**:134000 [Crossref], [Google Scholar], [Publisher]

[23]. Gandla K., Islam F., Zehravi M., Karunakaran A., Sharma I., Haque M.A., Kumar S., Pratyush K., Dhawale S.A., Nainu F., Natural polymers as potential P-glycoprotein inhibitors: Pre-ADMET profile and computational analysis as a proof of concept to fight multidrug resistance in cancer, *Heliyon*, 2023, **9** [Google Scholar], [Publisher]
[24]. Khan A., Unnisa, A., Sohel M., Date M., Panpaliya N., Saboo S.G., Siddiqui F., Khan S., Investigation of phytoconstituents of Enicostemma littorale as potential glucokinase activators through molecular docking for the treatment of type 2 diabetes mellitus, *In Silico Pharmacology*, 2021, **10**:1 [Crossref], [Google Scholar], [Publisher]
[25]. Morak-Młodawska B., Jeleń M., Martula E., Korlacki R., Study of lipophilicity and ADME properties of 1, 9-diazaphenothiazines with anticancer action, *International Journal of Molecular Sciences*, 2023, **24**:6970 [Crossref], [Google Scholar], [Publisher]
[26]. Waring M.J., Lipophilicity in drug discovery, *Expert Opinion on Drug Discovery*, 2010, **5**:235 [Crossref], [Google Scholar], [Publisher]
[27]. Lobo S., Is there enough focus on lipophilicity in drug discovery?, *Expert Opinion on Drug Discovery*, 2020, **15**:261 [Crossref], [Google Scholar], [Publisher]
[28]. Bickerton G.R., Paolini G.V., Besnard J., Muresan S., Hopkins A.L., Quantifying the chemical beauty of drugs, *Nature Chemistry*, 2012, **4**:90 [Crossref], [Google Scholar], [Publisher]
[29]. Kosugi T., Ohue M., Quantitative estimate index for early-stage screening of compounds targeting protein-protein interactions, *International Journal of Molecular Sciences*, 2021, **22**:10925 [Crossref], [Google Scholar], [Publisher]
[30]. Ursu O., Rayan A., Goldblum A., Oprea T.I., Understanding drug-likeness, *Wiley Interdisciplinary Reviews: Computational Molecular Science*, 2011, **1**:760 [Crossref], [Google Scholar], [Publisher]
[31]. Walters W.P., Going further than Lipinski's rule in drug design, *Expert Opinion on Drug Discovery*, 2012, **7**:99 [Crossref], [Google Scholar], [Publisher]
[32]. Johnson T.W., Dress K.R., Edwards M., Using the golden triangle to optimize clearance and oral absorption, *Bioorganic & Medicinal Chemistry Letters*, 2009, **19**:5560 [Crossref], [Google Scholar], [Publisher]
[33]. Lee J.B., Zgair A., Taha D.A., Zang X., Kagan L., Kim T.H., Kim M.G., Yun H., Fischer P.M., Gershkovich P., Quantitative analysis of lab-to-lab variability in Caco-2 permeability assays, *European Journal of Pharmaceutics and Biopharmaceutics*, 2017, **114**:38 [Crossref], [Google Scholar], [Publisher]
[34]. Feng B., West M., Patel N.C., Wager T., Hou X., Johnson J., Tremaine L., Liras J., Validation of human MDR1-MDCK and BCRP-MDCK cell lines to improve the prediction of brain penetration, *Journal of Pharmaceutical Sciences*, 2019, **108**:2476 [Crossref], [Google Scholar], [Publisher]
[35]. Persidsky Y., Ramirez S.H., Haorah J., Kanmogne G.D., Blood–brain barrier: structural components and function under physiologic and pathologic conditions, *Journal of Neuroimmune Pharmacology*, 2006, **1**:223 [Crossref], [Google Scholar], [Publisher]
[36]. Khan S.L., Sonwane G.M., Siddiqui F.A., Jain S.P., Kale M.A., Borkar V.S., Discovery of naturally occurring flavonoids as human cytochrome P450 (CYP3A4) inhibitors with the aid of computational chemistry, *Indo Glob. J. Pharm. Sci*, 2020, **10**:58 [Crossref], [Google Scholar], [Publisher]
[37]. Ogu C.C., Maxa J.L., Drug interactions due to cytochrome P450, *Baylor University Medical Center Proceedings, 2000,* 421 [Crossref], [Google Scholar], [Publisher]
[38]. Pan X., Mutagenicity Evaluation of Nanoparticles by the Ames Assay, *Environmental Toxicology and Toxicogenomics: Principles, Methods, and Applications*, 2021, 275 [Crossref], [Google Scholar], [Publisher]
[39]. Garg R., Smith C.J., Predicting the bioconcentration factor of highly hydrophobic organic chemicals, *Food and Chemical Toxicology*, 2014, **69**:252 [Crossref], [Google Scholar], [Publisher]
[40]. Arnot J.A., Gobas F.A., A review of bioconcentration factor (BCF) and

bioaccumulation factor (BAF) assessments for organic chemicals in aquatic organisms, *Environmental Reviews*, 2006, **14**:257 [Crossref], [Google Scholar], [Publisher]
[41]. Martin T.M., Young D.M., Prediction of the acute toxicity (96-h LC50) of organic compounds to the fathead minnow (Pimephales promelas) using a group contribution method, *Chemical Research in Toxicology*, 2001, **14**:1378 [Crossref], [Google Scholar], [Publisher]
[42]. Tkaczyk A., Bownik A., Dudka J., Kowal K., Ślaska B., Daphnia magna model in the toxicity assessment of pharmaceuticals: A review, *Science of the Total Environment*, 2021, **763**:143038 [Crossref], [Google Scholar], [Publisher]
[43]. Ezugwu J.A., Okoro U.C., Ezeokonkwo M.A., Hariprasad K.S., Rudrapal M., Gogoi N., Chetia D., Ugwu D.I., Eze F.U., Onyeyilim L.E., Design, synthesis, molecular docking, drug-likeness/ADMET and molecular dynamics studies of thiazolyl benzenesulfonamide carboxylates as antimalarial agents, *Chemistry Africa*, 2024, 1 [Crossref], [Google Scholar], [Publisher]
[44]. Sabarees G., Velmurugan V., Solomon V.R., Molecular docking and molecular dynamics simulations discover curcumin analogs as potential wound healing agents, *Chemical Physics Impact*, 2024, **8**:100441 [Crossref], [Google Scholar], [Publisher]
[45]. Astuti E., Raharjo T.J., Manalu P.B., Putra I.S., Waskitha S.S., Solin J., Synthesis, molecular docking, and evaluation of some new curcumin analogs as antimalarial agents, *Indonesian Journal of Chemistry*, 2021, **21**:452 [Google Scholar], [Publisher]
[46]. Nisa S.A., Jumina J., Mardjan M.I.D., Kurniawan Y.S., Synthesis, activity test and molecular docking of novel nitrophenylcalix [4]-2-methylresorcinarene derivatives as antimalarial agent, *Molekul*, 2023, **18**:404 [Crossref], [Google Scholar], [Publisher]
[47]. Hollingsworth S.A., Dror R.O., Molecular dynamics simulation for all, *Neuron*, 2018, **99**:1129 [Google Scholar], [Publisher]
[48]. Mohan M., Pramada S., Molecular dynamic simulations of the desalination process through membrane technology: A review, *Water Supply*, 2023, **23**:2773 [Crossref], [Google Scholar], [Publisher]
[49]. Sargsyan K., Grauffel C., Lim C., How molecular size impacts RMSD applications in molecular dynamics simulations, *Journal of Chemical Theory and Computation*, 2017, **13**:1518 [Crossref], [Google Scholar], [Publisher]
[50]. Duay S.S., Yap R.C.Y., Gaitano III A.L., Santos J.A.A., Macalino S.J.Y., Roles of virtual screening and molecular dynamics simulations in discovering and understanding antimalarial drugs, *International Journal of Molecular Sciences*, 2023, **24**:9289 [Crossref], [Google Scholar], [Publisher]
[51]. Chagaleti B.K., Kumar B.S., Rajagopal R., Alfarhan A., Arockiaraj J., Kumaradoss K.M., Namasivayam S.K.R., Targeting cyclin-dependent kinase 2 CDK2: Insights from molecular docking and dynamics simulation-a systematic computational approach to discover novel cancer therapeutics, *Computational Biology and Chemistry*, 2024, 108134 [Crossref], [Google Scholar], [Publisher]
[52]. Paul R.K., Ahmad I., Patel H., Kumar V., Raza K., Phytochemicals from Amberboa ramosa as potential DPP-IV inhibitors for the management of Type-II diabetes mellitus: Inferences from in-silico investigations, *Journal of Molecular Structure*, 2023, **1271**:134045 [Crossref], [Google Scholar], [Publisher]
[53]. Ahmad I., Akand S.R., Shaikh M., Pawara R., Manjula S., Patel H., Synthesis, molecular modelling study of the methaqualone analogues as anti-convulsant agent with improved cognition activity and minimized neurotoxicity, *Journal of Molecular Structure*, 2022, **1251**:131972 [Crossref], [Google Scholar], [Publisher]
[54]. Pawara R., Ahmad I., Nayak D., Belamkar S., Surana S., Kundu C.N., Patil C., Patel H., Design and synthesis of the novel, selective WZ4002 analogue as EGFR-L858R/T790M tyrosine kinase inhibitors for targeted drug therapy in non-small-cell lung cancer (NSCLC), *Journal of Molecular Structure*, 2022, **1254**:132313 [Crossref], [Google Scholar], [Publisher]
[55]. Acar Çevik U., Celik I., Işık A., Ahmad I., Patel H., Özkay Y., Kaplancıklı Z.A., Design, synthesis, molecular modeling, DFT, ADME and biological

evaluation studies of some new 1, 3, 4-oxadiazole linked benzimidazoles as anticancer agents and aromatase inhibitors, *Journal of Biomolecular Structure and Dynamics*, 2023, **41**:1944 [Crossref], [Google Scholar], [Publisher]

[56]. Girase R., Ahmad I., Pawara R., Patel H., Optimizing cardio, hepato and phospholipidosis toxicity of the Bedaquiline by chemoinformatics and molecular modelling approach, *SAR and QSAR in Environmental Research*, 2022, **33**:215 [Crossref], [Google Scholar], [Publisher]

HOW TO CITE THIS ARTICLE

K.T. Kumar Reddy, U.V. Naga Venkata Arjun, J.F. Alhmoud, S.M. Reddy, D. D., V.B. Tambe, G.S. Shinde, T.S. Shanmugarajan, G. Dharmamoorthy, G. P. In Depth *in Silico* Exploration of Some Natural Indole Alkaloids as Potential Plasmepsin II Inhibitors: ADMET Calculations, Molecular Docking Analysis, Molecular Dynamics Simulation, and DFT Studies. *Chem. Methodol.*, 2025, 9(4) 277-300

DOI: https://doi.org/10.48309/CHEMM.2025.500292.1884

URL: https://www.chemmethod.com/article_216261.html